

MR Imaging of the Normal Meninges: Comparison of Contrast-Enhancement Patterns on 3D Gradient-Echo and Spin-Echo Images

James W. Farn¹
Scott A. Mirowitz

OBJECTIVE. The purpose of this study was to determine the enhancement pattern of the normal meninges on T1-weighted three-dimensional Fourier transform gradient-echo (3DGE) MR images and to compare this pattern with that observed on conventional two-dimensional Fourier transform spin-echo (2DSE) images. This will serve as a basis for comparison when cases of suspected meningeal pathology are evaluated.

SUBJECTS AND METHODS. The appearance of the normal meninges after administration of gadopentetate dimeglumine was evaluated on 2DSE and 3DGE images in 69 patients who had no known or suspected meningeal abnormality. The total percentage of meningeal surface area that underwent contrast enhancement and the continuity of meningeal enhancement were evaluated at four anatomic levels.

RESULTS. In most patients, 2DSE images showed short segments (i.e., <3 cm) of meningeal enhancement, with enhancement of less than 50% of total meningeal surface area. However, enhancement of 76–100% of total meningeal surface area was routinely observed on 3DGE images, with long segments (i.e., >3 cm) or continuous patterns most frequently observed. The differences between 2DSE and 3DGE sequences were statistically significant for all regions that were assessed.

CONCLUSION. Continuous meningeal enhancement or enhancement of long segments of normal meninges is routinely observed on contrast-enhanced 3DGE images; this appearance differs from those of enhanced 2DSE images and should not be interpreted as abnormal.

AJR 1994;162:131–135

Three-dimensional Fourier transform gradient-echo (3DGE) MR imaging has certain advantages over conventional two-dimensional spin-echo (2DSE) MR imaging, including increased spatial resolution and improved visibility of susceptibility and flow effects with no sacrifice in its sensitivity for depicting lesion contrast enhancement [1–3]. For these reasons, contrast-enhanced 3DGE imaging is used as a problem-solving technique at our institution. When these images were reviewed, it was frequently noted that the meningeal enhancement patterns on 2DSE and 3DGE images differed significantly. The objective of this study was to compare contrast enhancement of normal meninges on images obtained with the two techniques.

Subjects and Methods

The initial study group consisted of 93 randomly selected patients who underwent cranial MR imaging. Twenty-four patients were eliminated from the study because they had a history of photophobia, meningitis, cortical infarcts, previous cranial surgery, or metastatic disease or the presence of enhancing intracranial lesions. The remaining 69 patients consisted of 46 women and 23 men (22–89 years old; mean age, 60 years) with no clinical evidence of meningeal abnormality or of conditions that are known to predispose to abnormal contrast enhancement of the meninges on MR images.

Received July 14, 1993; accepted after revision September 8, 1993.

¹Both authors: Mallinckrodt Institute of Radiology (Jewish Hospital), Washington University School of Medicine, 216 S. Kingshighway Blvd., St. Louis, MO 63110. Address correspondence to S. A. Mirowitz.

0361-803X/94/1621-0131
© American Roentgen Ray Society

Imaging was performed on a 1.5-T (Signa, General Electric) system. Sagittal T1-weighted (433/11 [TR/TE], two excitations) and axial proton density-weighted and T2-weighted (3000/30,95, one excitation) images were initially obtained. T1-weighted (500/11, two excitations) 2DSE axial images were then acquired before and after IV administration of 0.1 mmol/kg of gadopentetate dimeglumine. T1-weighted 3DGE images (38/5, one excitation, 45° flip angle, 64 partitions) were then obtained by using a spoiled gradient-recalled acquisition in the steady state (GRASS) sequence. In 10 patients, 3DGE images were acquired before and after administration of contrast material. In an additional 10 patients, 3DGE images were acquired before 2DSE images. 2DSE images were acquired by using a 5-mm slice thickness and 1-mm interslice gap. 3DGE images were of 2 mm thickness with no intervening gap. An imaging matrix of 256 (frequency) \times 192 (phase) was used for all sequences.

The meningeal enhancement pattern was evaluated at four anatomic levels in all patients. These included images acquired in the region of the fourth ventricle (level one), the temporal horns (level two), the body of the lateral ventricles (level three), and the centrum semiovale (level four) (Fig. 1). The enhancement pattern of the falx cerebri at level three was also assessed. Two radiologists jointly evaluated the images for the total percentage of meningeal enhancement and for continuity of meningeal enhancement. They were aware of sequence type because of the obvious differences between the images. Total percentage meningeal enhancement was determined by identifying segments of meningeal enhancement at each level and estimating the sum of these enhancing segments relative to total meningeal surface area. Results were categorized as no enhancement, 1–25%, 26–50%, 51–75%, 76–99%, or 100% meningeal enhancement. Continuity of enhancement was determined by selecting the longest uninterrupted segment of meningeal enhancement at each level and categorizing it as no enhancement, short segment (less than 3 cm), long segment (equal to or greater than 3 cm), or continuous.

Results were analyzed by using two-tailed t-tests, with significance defined at the $p < .05$ level.

Results

Results are summarized in Tables 1 and 2. The length and continuity of meningeal enhancement were least extensive on images that were acquired through the posterior fossa (level one). At this level, total percentage enhancement of the meninges was estimated at 1–25% in 79% of patients on 2DSE images and in 42% of patients on 3DGE images. Fewer patients had enhancement of more than 75% of total meningeal surface area observed on 3DGE images at this level than at any other level. Regarding continuity of

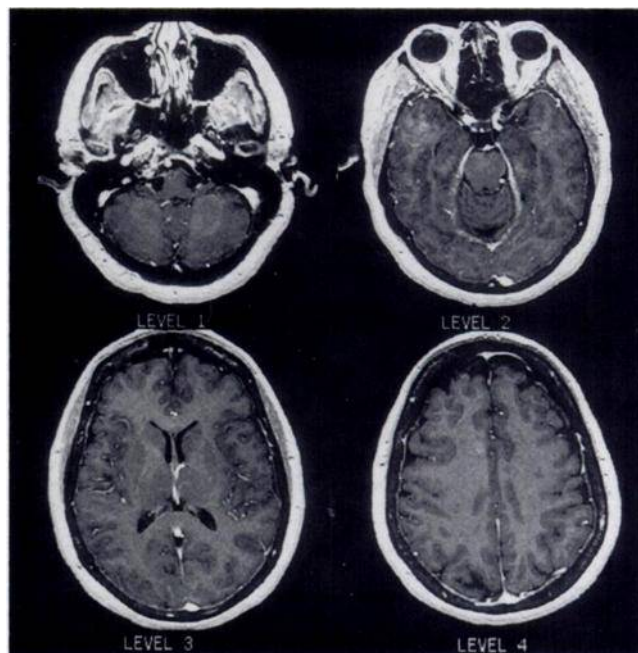


Fig. 1.—Contrast-enhanced 3DGE images of a patient with normal meninges. Images show levels that were evaluated for meningeal enhancement. These include infratentorial (level one; upper left), temporal lobes (level two; upper right), level of the lateral ventricles (level three; lower left), and supraventricular (level four; lower right). Fine linear enhancement can be seen throughout most of meningeal surfaces at all levels.

enhancement, the most frequent finding was “short segment enhancement” on 2DSE (88% of patients) and 3DGE (50% of patients) images. This was the only level at which a majority of patients did not show either long-segment or continuous meningeal enhancement on 3DGE images.

At level two, enhancement of 1–25% of total meningeal surface area was observed in most patients (55%) on 2DSE images; most remaining patients showed between 26% and 50% total meningeal enhancement. On 3DGE images, most patients (88%) showed 76–100% enhancement (Fig. 2). Enhancement of a short segment of meninges was observed in most patients (71%) on 2DSE images at this level, whereas 3DGE images showed enhancement that was either continuous (52%) or involved long segments (48%).

TABLE 1: Total Percentage Meningeal Enhancement on Contrast-Enhanced 2DSE and 3DGE MR Images

| Level | 0% | | 1–25% | | 26–50% | | 51–75% | | 76–99% | | 100% | |
|-------|------|------|-------|------|--------|------|--------|------|--------|------|------|------|
| | 2DSE | 3DGE | 2DSE | 3DGE | 2DSE | 3DGE | 2DSE | 3DGE | 2DSE | 3DGE | 2DSE | 3DGE |
| 1 | 9 | 4 | 79 | 42 | 9 | 12 | 3 | 26 | 0 | 12 | 0 | 4 |
| 2 | 0 | 0 | 55 | 0 | 32 | 0 | 12 | 12 | 1 | 49 | 0 | 39 |
| 3 | 1 | 0 | 27 | 0 | 49 | 3 | 19 | 7 | 3 | 52 | 1 | 38 |
| 4 | 1 | 0 | 85 | 0 | 13 | 3 | 1 | 14 | 0 | 40 | 0 | 43 |
| Falx | 4 | 0 | 31 | 0 | 14 | 3 | 14 | 6 | 13 | 10 | 23 | 81 |

Note.—2DSE = two-dimensional spin-echo, 3DGE = three-dimensional gradient-recalled echo. All numbers indicate percentage of patients.

TABLE 2: Maximum Length of Uninterrupted Meningeal Enhancement on Contrast-Enhanced 2DSE and 3DGE MR Images

| Level | None | | Short Segment | | Long Segment | | Continuous | |
|-------|------|------|---------------|------|--------------|------|------------|------|
| | 2DSE | 3DGE | 2DSE | 3DGE | 2DSE | 3DGE | 2DSE | 3DGE |
| 1 | 9 | 4 | 88 | 50 | 3 | 32 | 0 | 14 |
| 2 | 0 | 0 | 71 | 0 | 29 | 48 | 0 | 52 |
| 3 | 0 | 0 | 61 | 1 | 38 | 38 | 1 | 61 |
| 4 | 0 | 0 | 97 | 1 | 3 | 37 | 0 | 62 |
| Falx | 4 | 0 | 51 | 10 | 7 | 9 | 38 | 81 |

Note.—2DSE = two-dimensional spin-echo, 3DGE = three-dimensional gradient-recalled echo. All numbers indicate percentage of patients.

At level three, the most frequent observation regarding total percentage meningeal enhancement was 26–50% enhancement (49% of patients) on 2DSE images and 76–99% enhancement (52% of patients) on 3DGE images (Fig. 3). Most patients (61%) showed enhancement of short segments of meninges on 2DSE images, with continuous

meningeal enhancement most frequently observed on 3DGE images (61%).

At level four, the vast majority of patients (85%) showed enhancement of 1–25% of total meningeal surface area on 2DSE images, whereas 76–100% enhancement was observed in a similar percentage of patients (83%) on 3DGE images. 2DSE images again showed enhancement of short segments of meninges in virtually all patients (97%) at this level. The meningeal enhancement pattern observed on 3DGE images was continuous (62%) or involved long segments (37%; Fig. 4).

Total percentage enhancement of the falx cerebri on 3DGE images showed the greatest number of patients (81%) to have 100% enhancement. The most frequent finding regarding continuity of enhancement on 2DSE images was “short segment” (51% of patients). 3DGE images at this level showed enhancement to be most frequently continuous (81% of patients).

Differences between 2DSE and 3DGE images regarding total percentage meningeal enhancement and the continuity (i.e., pattern) of meningeal enhancement were highly significant ($p < .01$) for all anatomic regions.

Fig. 2.—Corresponding contrast-enhanced 2DSE (A) and 3DGE (B) MR images at level of temporal horns (level two) of a patient with normal meninges. Short interrupted segments of meningeal enhancement are observed on 2DSE image (arrows), compared with more continuous enhancement throughout meninges on 3DGE image (arrows).

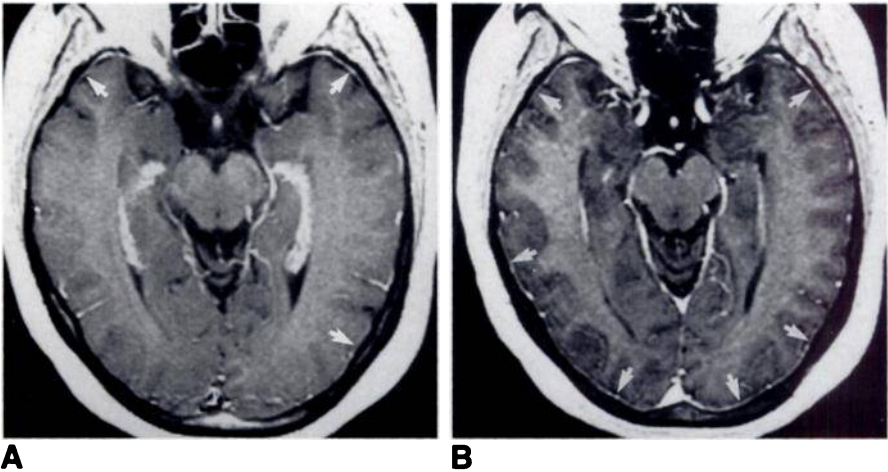
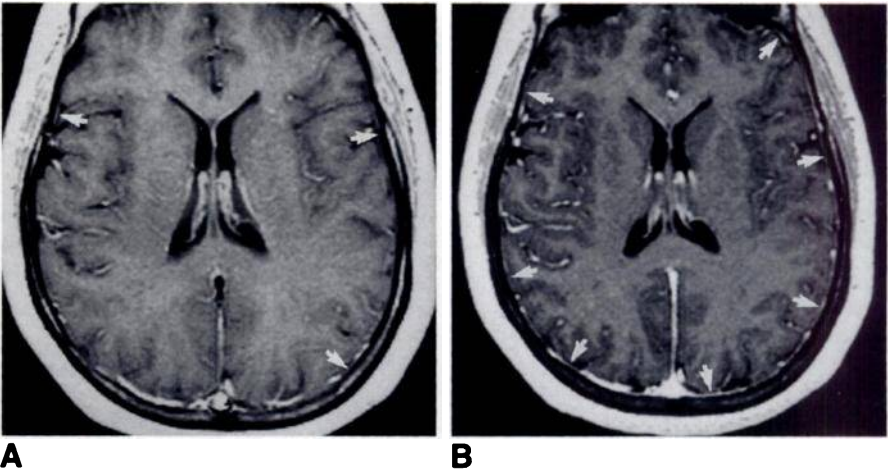


Fig. 3.—Corresponding contrast-enhanced 2DSE (A) and 3DGE (B) MR images at level of lateral ventricles (level three) of a patient with normal meninges. Short interrupted segments of meningeal enhancement are seen on 2DSE image (arrows), compared with more continuous enhancement throughout meninges on 3DGE image (arrows).



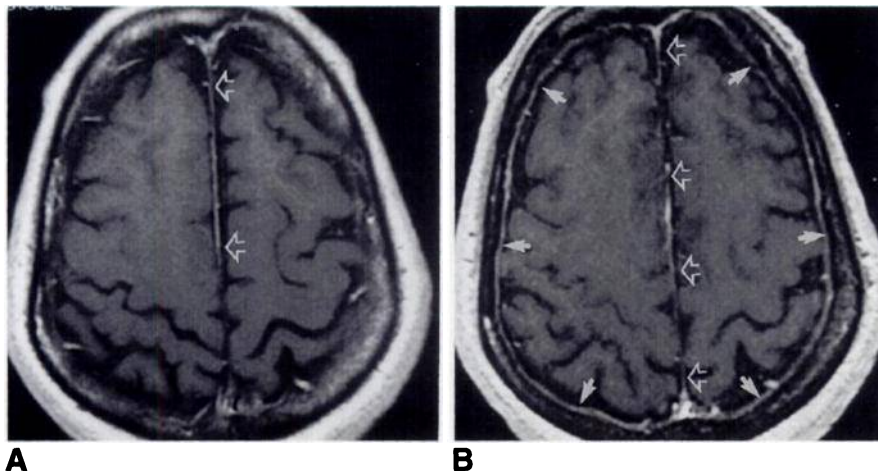


Fig. 4.—Corresponding contrast-enhanced 2DSE (A) and 3DGE (B) MR images at level of supraventricular white matter (level four) of a patient with normal meninges. Minimal meningeal enhancement is seen on 2DSE MR image, whereas 3DGE MR image shows continuous enhancement throughout meninges (closed arrows in B). Also note increased length of enhancement of falx cerebri (open arrows) and relative decreased signal intensity of diploic space on 3DGE image.

In the 10 patients in whom contrast-enhanced 3DGE images were acquired before 2DSE images, significantly greater total percentage meningeal enhancement and continuity of meningeal enhancement were observed on 3DGE images, with findings similar to those observed in the population described earlier.

Discussion

The normal meninges appear as thin short areas of relatively low signal intensity on unenhanced 2DSE images. After IV administration of paramagnetic contrast material, the meninges that overlie the cerebrum exhibit fine linear enhancement in a short segmental pattern [4]. The falx and tentorium show enhancement after contrast administration in approximately 50% of patients [5], again usually in a short segmental pattern. The pattern of normal meningeal enhancement on 2DSE images in our study was consistent with that described in previous reports and was characterized by thin, linear, short segments of enhancement in nearly all patients.

Meningeal enhancement patterns on 2DSE images that are suggestive of abnormality include increased intensity and length of meningeal enhancement, as well as associated nodularity. These characteristics may be observed in association with meningioma, meningeal carcinomatosis [5], primary intracranial neurogenic tumors [6], and meningitis [7], as well as in patients who have undergone extraaxial hemorrhage or previous cranial surgery [8]. These characteristics are not routinely seen on contrast-enhanced 2DSE images in patients with normal meninges.

However, our study indicates that contrast-enhanced 3DGE images display some of these features in patients who do not have abnormal meninges. We observed a significant increase in the continuity of meningeal enhancement, as well as a significantly greater total percentage of meningeal enhancement on enhanced 3DGE images compared with 2DSE images (Fig. 2). The meninges surrounding the cerebrum, for example, displayed total meningeal enhancement on 2DSE images that was less than 50% in most patients, whereas total meningeal enhancement on

3DGE images in this region was more than 75% in most patients. 2DSE images showed short-segment meningeal enhancement in most patients, whereas 3DGE images showed long-segment or continuous meningeal enhancement in nearly all patients. Our findings indicate that the increased length and continuity of meningeal enhancement on 3DGE images compared with 2DSE images should, therefore, be considered normal.

At the level of the cerebellum, we found a significant increase in length and continuity of meningeal enhancement on 3DGE images compared with the corresponding 2DSE images. However, these differences were not as pronounced as at higher levels. This is attributed to prominent contrast enhancement of the transverse sinus, which results in decreased conspicuousness of adjacent meningeal enhancement in the posterior fossa on both 2DSE and 3DGE images (Fig. 3). In addition, because of the relatively decreased cerebellar surface area compared with the cerebrum, the length of 3 cm (the length used to differentiate short- and long-segment enhancement in this study) may be too great to visualize smaller differences in absolute length in this region.

The alterations in appearance of meningeal enhancement on 2DSE and 3DGE images reflect several differences between these two pulse sequences. The 3DGE technique we used had considerably smaller slice thickness than our 2DSE sequence and, furthermore, had no interslice gap. These factors combine to improve spatial resolution and to decrease partial volume averaging, and they most likely contributed to the greater conspicuousness of meningeal enhancement on 3DGE images than on 2DSE images. Another factor that probably contributes to increased conspicuousness of meningeal enhancement on 3DGE images is the relatively decreased signal intensity of the diploë on 3DGE compared with 2DSE images (Fig. 2). This is a result of accentuation of susceptibility effects at trabecular bone–bone marrow interfaces, which are present on gradient-echo images because the 180° refocusing pulse is absent. The relatively reduced signal intensity of the diploë allows improved visualization of enhancement of the adjacent meninges. The increased sensitivity of gradient-echo images to blood flow may further increase the conspicuousness of meningeal enhancement on

these images, as the meninges contain multiple vascular structures. Although our acquisition of 3DGE images after the 2DSE images in most patients in our study introduces some bias, it is not thought to be a significant factor in the discrepant enhancement patterns we observed. This was verified in the subpopulation of 10 patients in whom this acquisition order was reversed, with results similar to those obtained in the remainder of the study group.

In conclusion, we have found that the enhancement pattern of the normal meninges differs on 2DSE and 3DGE images. 3DGE images show greater total meningeal enhancement and greater continuity of meningeal enhancement than do conventional 2DSE images. This appearance is attributed to multiple technical differences between these two pulse sequences, as discussed earlier. The observation of continuous meningeal enhancement on 3DGE images, in the absence of associated meningeal thickening or nodularity, should be recognized as normal. Awareness of these normal findings is important in the accurate interpretation of contrast-enhanced 3DGE images.

REFERENCES

1. Frahm J, Haasse A, Matthaei D. Rapid three-dimensional MR imaging using the FLASH technique. *J Comput Assist Tomogr* **1986**;10:363-368
2. Runge VM, Wood ML, Kaufman DM, Nelson KL, Trail MR. FLASH: clinical three-dimensional magnetic resonance imaging. *RadioGraphics* **1988**;8: 947-965
3. Mirowitz SA. Intracranial lesion enhancement with gadolinium: T1-weighted spin-echo versus three-dimensional Fourier transform gradient-echo MR imaging. *Radiology* **1992**;185:1-5
4. Kilgore DP, Breger RK, Daniels DL, Pojunas KW, Williams AL, Haughton VM. Cranial tissues: normal MR appearance after intravenous injection of Gd-DTPA. *Radiology* **1986**;159:757-761
5. Sze G, Soletsky S, Bronen R, Krol G. MR imaging of the cranial meninges with emphasis on contrast enhancement and meningeal carcinomatosis. *AJNR* **1989**;10:965-975
6. Berry I, Brant-Zawadzki M, Osaki L, Brasch R, Murovic J, Newton T. Gd-DTPA in clinical MR of the brain: 2. Extraaxial lesions and normal structures. *AJNR* **1986**;7:789-793
7. Chang KH, Han MH, Roh JK, Kim IO, Han MC, Kim CW. Gd-DTPA-enhanced MR imaging of the brain in patients with meningitis: comparison with CT. *AJR* **1988**;151:809-816
8. Burke JW, Podrasky AE, Bradley WG. Meninges: benign postoperative enhancement of MR images. *Radiology* **1990**;74:99-102

This article has been cited by:

1. Nora Navina Sommer, Romina Pons Lucas, Eva Coppenrath, Hendrik Kooijman, Franziska Galiè, Nina Hesse, Wieland H. Sommer, Karla M. Treitl, Tobias Saam, Matthias F. Froelich. 2020. Contrast-enhanced modified 3D T1-weighted TSE black-blood imaging can improve detection of infectious and neoplastic meningitis. *European Radiology* 30:2, 866-876. [[Crossref](#)]
2. Fumiaki Ueda, Miho Okuda, Hiroyuki Aburano, Yuichi Yoshie, Osamu Matsui, Toshifumi Gabata. 2017. Cranial Pachymeningeal Involvement in POEMS Syndrome: Evaluation by Pre- and Post-contrast FLAIR and T1-weighted Imaging. *Magnetic Resonance in Medical Sciences* 16:3, 231-237. [[Crossref](#)]
3. STEPHEN JOSLYN, MARTIN SULLIVAN, ROSA NOVELLAS, NICOLA BRENNAN, GILL CAMERON, GAWAIN HAMMOND. 2011. EFFECT OF DELAYED ACQUISITION TIMES ON GADOLINIUM-ENHANCED MAGNETIC RESONANCE IMAGING OF THE PRESUMABLY NORMAL CANINE BRAIN. *Veterinary Radiology & Ultrasound* 52:6, 611-618. [[Crossref](#)]
4. Neel Patel, Olga Kirimi. 2009. Anatomy and Imaging of the Normal Meninges. *Seminars in Ultrasound, CT and MRI* 30:6, 559-564. [[Crossref](#)]
5. Melanie B. Fukui, Carolyn Cidis Meltzer. Meningeal Processes 399-428. [[Crossref](#)]
6. Julie-Marthe Grenier, Michelle A. Wessely. 2007. Magnetic resonance imaging of the spinal cord. *Clinical Chiropractic* 10:4, 205-217. [[Crossref](#)]
7. D. Reizine, J.-P. Guichard, G. Jourdan, O. Belhocine. 2006. Barrière hématoencéphalique. *EMC - Radiologie et imagerie médicale - Musculosquelettique - Neurologique - Maxillofaciale* 1:1, 1-9. [[Crossref](#)]
8. Linda M. Mellema, Valerie F. Samii, Karen M. Vernau, Richard A. Lecouteur. 2002. MENINGEAL ENHANCEMENT ON MAGNETIC RESONANCE IMAGING IN 15 DOGS AND 3 CATS. *Veterinary Radiology & Ultrasound* 43:1, 10-15. [[Crossref](#)]
9. Michael R Sage, Alan J Wilson, Rebecca Scroop. 2000. Contrast media and the brain. The basis of computed tomography and magnetic resonance imaging enhancement: A review. *Australasian Radiology* 44:2, 133-142. [[Crossref](#)]
10. Bahram Mokri, David G. Piepgras, Gary M. Miller. 1997. Syndrome of Orthostatic Headaches and Diffuse Pachymeningeal Gadolinium Enhancement. *Mayo Clinic Proceedings* 72:5, 400-413. [[Crossref](#)]
11. M Braun, S Bracard, J-C Huot, J Roland, L Picard. 1996. Pontine veins. MRI cross-sectional anatomy. *Surgical and Radiologic Anatomy* 18:4, 315-321. [[Crossref](#)]
12. M. Braun, S. Bracard, R. Anxionnat, J. Roland, L. Picard. 1996. The veins of the medulla oblongata: MRI cross-sectional anatomy. *Surgical and Radiologic Anatomy* 18:3, 201-207. [[Crossref](#)]
13. Rona Woldenberg Greenberg, Elizabeth L. Lane, Jay Cinnamon, Peter Farmer, Roger A. Hyman. 1994. The cranial meninges: Anatomic considerations. *Seminars in Ultrasound, CT and MRI* 15:6, 454-465. [[Crossref](#)]
14. Jay Cinnamon, Mahendra Sharma, Daniel Gray, Rona Greenberg, Roger A. Hyman. 1994. Neuroimaging of meningeal disease. *Seminars in Ultrasound, CT and MRI* 15:6, 466-498. [[Crossref](#)]